Optical mapping of single-molecule human DNA in disposable, mass-produced all-polymer devices

OPEN ACCESS
IOP Publishing
Journal of Micromechanics and Microengineering
J. Micromech. Microeng. **25** (2015) 105002 (8pp)
doi:10.1088/0960-1317/25/10/105002

Optical mapping of single-molecule human DNA in disposable, mass-produced all-polymer devices

Peter Friis Østergaard[1,3], Joanna Lopacinska-Jørgensen[2,3], Jonas Nyvold Pedersen[1], Niels Tommerup[2], Anders Kristensen[1], Henrik Flyvbjerg[1], Asli Silahtaroglu[2], Rodolphe Marie[1] and Rafael Taboryski[1]

[1] Department of Micro- and Nanotechnology, Technical University of Denmark, DK-2800 Kgs. Lyngby, Denmark
[2] Department of Cellular and Molecular Medicine, Faculty of Health and Medical Sciences, University of Copenhagen, Copenhagen, Denmark

E-mail: asli@sund.ku.dk, rodolphe.marie@nanotech.dtu.dk and rafael.taboryski@nanotech.dtu.dk

Received 26 April 2015, revised 16 July 2015
Accepted for publication 22 July 2015
Published 26 August 2015

Abstract

We demonstrate all-polymer injection molded devices for optical mapping of denaturation–renaturation (DR) patterns on long, single DNA-molecules from the human genome. The devices have channels with ultra-low aspect ratio, only 110 nm deep while 20 μm wide, and are superior to the silica devices used previously in the field. With these polymer devices, we demonstrate on-chip recording of DR images of DNA-molecules stretched to more than 95% of their contour length. The stretching is done by opposing flows Marie *et al* (2013 *Proc. Natl Acad. Sci. USA* **110** 4893–8). The performance is validated by mapping 20 out of 24 Mbp-long DNA fragments to the human reference genome. We optimized fabrication of the devices to a yield exceeding 95%. This permits a substantial economies-of-scale driven cost-reduction, leading to device costs as low as 3 USD per device, about a factor 70 lower than the cost of silica devices. This lowers the barrier to a wide use of DR mapping of native, megabase-size DNA molecules, which has a huge potential as a complementary method to next-generation sequencing.

Keywords: injection molding, human DNA mapping, lab-on-a-chip

S Online supplementary data available from stacks.iop.org/JMM/25/105002/mmedia

(Some figures may appear in colour only in the online journal)

1. Introduction

Optical mapping of individual DNA molecules has been proposed as a complement to next generation sequencing (NGS) [2–4] as it provides whole-genome ordered maps from fragments of individual genomic DNA molecules [5]. This method has supported NGS in the assembly of genomes of rice [6], certain bacteria [7], and a domestic goat [8] by providing long-range context for the NGS short read lengths, a technique known as scaffolding. Moreover, optical mapping of native, megabase-size DNA molecules can detect repetitive genomic regions and unique structural variations on its own [1]. Since optical mapping can work on a single-molecule level, differences between individual cells in a population can also be investigated using this technique, as ensemble averaging is not always required [9, 10]. For DR mapping, like other sequence-to-map techniques it can be proven mathematically that the probability of

[3] These authors contributed equally to the article.

aligning a DR map from a 100 kB DNA molecule to an incorrect position in the human reference genome is negligible [1, 11, 12]. Hence, there is no need for multifold coverage of the genome.

Optical mapping is done with fluorescently labelled and linearly stretched DNA molecules, which makes an optical 'barcode' visible along the molecule [9, 11]. One of the optical mapping techniques combines DNA stretching by entropic confinement with fluorescence imaging of denaturation patterns of the genomic DNA [13]. Recently an alternative stretching method, the so-called convex lens-induced nanoscale templating (CLINT) [14, 15] was proposed. It loads DNA molecules into nanochannels with no use of high pressures, but has only been demonstrated for fairly short molecules. For automated operation, however, pressure control or electrophoresis is preferable. State-of-the-art devices, as the one used by Marie *et al* [1], stretch long (~2 Mbp) DNA-molecules up to 98% of their contour lengths. This gives DR maps of the molecules with a resolution down to ~1 kbp.

Despite the successful performance of silica devices, their price is an obstacle for a more widespread use of optical mapping. Silica chips are fabricated only in small numbers, intended solely for a small community of highly specialized researchers and bearing a price tag of several hundred dollars per chip. With the aim of sequencing an entire human genome for 1.000 USD [16, 17], any supporting technique must be cheap [18, 19]. If high-performance chips can be fabricated as cheap plastic devices using industrial production methods, more researchers can benefit from DR-mapping. This is likely to boost the development of the technique, thereby releasing the full potential of optical mapping for aiding and validating present-day state-of-the-art NGS systems. Disposable systems furthermore have the advantage of removing the risk of cross contamination between experiments, which is essential for the analysis of human DNA.

Injection molding is an industry standard for production of consumer plastic products, but is also a good tool for replicating structures fabricated in silicon wafers [20, 21]. Such injection molded polymer lab-on-a-chip systems have previously been used for experiments with DNA, but these experiments have either been aimed at investigating the physical properties of homogeneously stained DNA [22], or mapping of consensus barcodes of smaller λ-DNA and T4GT7-DNA found by averaging data from many molecules [23].

Chip technologies comprising polydimethylsiloxane (PDMS) chips bonded to glass cover plates have been demonstrated and are commercially available [7, 8, 24]. However, as pointed out by Chantiwas *et al*, these technologies suffer from the serious drawbacks of 'roof collapse' for low aspect ratio nanoslits. Methods comprising nano-imprint lithography [25], and a combination of micro-molding and imprinting [26] have been demonstrated for optical mapping of short DNA.

Here we demonstrate the use of injection molded polymer nano-fluidic devices for optical DR mapping of megabase-size individual DNA-molecules from the human genome. Further we demonstrate an on-chip-handling protocol that avoids fragmentation of the DNA-molecules during handling. In particular, we demonstrate that the all-polymer devices can be injection molded and bonded with a final yield as high as 95%. This is considerably higher than the previously achieved 5–10% for polymer flow-stretch devices [27]. Furthermore, the autofluorescence was lowered by the addition of a masterbatch of a black dye to the polymer granulate used for injection molding of the devices. This reduced the background signal of the devices to nearly half the value obtained for transparent TOPAS devices, leading to an autofluorescence even lower than for silica devices. DR maps obtained from single human DNA-molecules are of sufficient quality to map against the whole human reference genome with the same mathematical procedure as is used for DR maps recorded in state-of-the-art silica devices, but now in polymer chips with a cost of only ~3 USD. Hence, when compared to silica devices [1], our chips are superior by featuring a factor of 70 cost reduction, and 20% lower autofluorescence.

One of the challenges of DNA preparation protocols is to avoid that DNA molecules fragment during handling. For silica chips, we have previously shown that all operations comprising DNA extraction, denaturation, renaturation, and stretching can be performed on-chip, allowing for a very gentle handling of DNA [1]. However, the negatively charged DNA molecules stick more easily to polymer surfaces than to silica surfaces [28] due to the less negative zeta-potential for polymeric surfaces compared to silica [29]. This considerably increases the risk of fragmenting during handling of long strands of DNA in polymer chips. Hence, in this work we developed and employed a modified protocol applicable for polymer chips to allow for the same on-chip operations as was used by Marie *et al* [1]. This greatly reduced the risk of fragmenting the long DNA molecules with the uncontrolled vigorous shear flow induced by pipetting the sample between sample tubes and chip.

2. Methods and materials

The melting-mapping technique was described by Reisner *et al* [11] while the working principle behind the shallow nanochannel (nanoslit) design was described by Marie *et al* [1]. Briefly, DNA is stained with the intercalating dye YOYO-1, followed by heating of the sample to a temperature between the melting points of the AT bonds and the GC bonds. This results in a partial denaturation of the molecule, in which the weaker adenine–thymine (AT) base pair bonds break, while the stronger guanine–cytosine (GC) bonds remain intact. This releases the fluorophores in the denatured AT-rich regions. When the sample is cooled, the AT-rich regions renature, but without intercalating fluorophores—they were lost when released. Next, opposing flows stretch the DNA in the nanoslit, which makes the local concentration of YOYO-1 visible by fluorescent microscopy. The pattern of fluorescence intensity along the DNA that is obtained in this manner is subsequently compared to a theoretical profile calculated from a reference genome. In the cross-shaped design of the nanoslit used for this technique, opposite flows over the DNA molecule are established to induce a tension in the pN range required to stretch DNA to nearly its contour length. This contrasts with

stretching by confinement alone where stretching beyond 80% requires advanced electron beam lithography and regrowth to create sub-50 nm channels [30, 31], or extreme ionic conditions [32].

2.1. Chip fabrication

A microfluidic system with a layout as shown in figure 1(a)) was fabricated using dry etching, electroplating and molding [20] similarly to the one described by Tanzi *et al* [27]. The overall chip layout was defined by the injection molding tool used and consisted of a 2 mm thick base plate of diameter 50 mm fitted with 12 integrated Luer connectors. The Luer connecters are placed in an array 9 mm apart from each other. A 4 cm^2 area without Luer ports is present to accommodate delicate structures and ease of microscopy [33]. Functional devices used for patch clamping of cells have previously been fabricated using this method [34], but in the present devices, the dimensions of the critical structures are significantly smaller. Briefly, the device fabrication comprises the following steps: a master silicon wafer is produced using thermal oxide growth, standard UV lithography, and RIE etch. This silicon master is electroplated in a nickel bath and the resulting nickel insert is used for injection molding of the polymer chips. This entire process is sketched in figure 1(b)).

Injection molding of the devices is done with an Engel Victory 80/45 Tech machine, using COC TOPAS grade 5013L-10 granulate from TOPAS Advanced Polymers GmbH. For black polymer devices, 2% (w/w) of black UNS 949 227 masterbatch from Gabriel Chemie GmbH is added to the polymer granulate. The cycle time of the injection molding is 90 s per device, everything included.

Standard LUER ports are integrated into the injection molding tool, making it easy to connect the final device with equipment such as pressure controllers [33].

The critical improvement to the fabrication scheme is the bonding protocol which gave a yield of 95%, compared to 5–10% in our previous work [27]. The devices are bonded in a UV-assisted thermal bonding process [35]. The polymer device and a piece of 150 μm thick TOPAS COC 5013L-10 foil is exposed to UV light for 30 s before thermal bonding. The surfaces of both the foil and the 2 mm thick sample were exposed to a UV lamp (DYMAX mercury UV-bulb F/5000) emitting over the full unfiltered Hg line spectrum with a power of 44.5 W cm^{-2} measured at the wavelength of 365 nm. This irradiance was measured at the sample position; ca. 10 cm. from the lamp. The two pieces are placed with the irradiated surfaces against each other, and a specially designed PDMS slab is placed on top of it. The PDMS slab contains cavities with a diameter of 3 mm over the low aspect ratio structures in order to avoid collapse of these during the bonding. Polymer devices are positioned in a custom made holder that allows five chips to be bonded at the same time. Successful bonding required two steps: First, the devices were bonded for 5 min at 125 °C and 0.6 bar. Secondly, the PDMS slab was replaced with one containing cavities with a diameter of 1 cm over the nanoslit, and the devices were bonded for an additional 5 min at 125 °C and 1.3 bar. This procedure allows for a bonding throughput of 25 chips per hour. The final devices, transparent and black, are seen in figure 1(c)).

2.2. DNA preparation

All reagents were purchased from Sigma-Aldrich unless otherwise specified. Human chromosomal DNA in nuclei from cultured fibroblast cells of an anonymous donor was supplied in 0.6% agarose plugs. Preparation of cell nuclei in agarose plugs was based on a previously published method [36] with some modifications. The fibroblast cells were grown until confluence in Dulbecco's modified Eagle's medium with Glutamax (DMEM; GIBCO Life Technologies), 10% fetal bovine serum, and 1% penicillin-streptomycin (P/S; GIBCO Life Technologies). Cells were washed with 1 × PBS, dissociated with trypsin/EDTA and centrifuged at 1100 rpm for 3 min. The supernatant was discarded and cells were resuspended in freshly prepared ice-cold nuclei isolation buffer (10 mM Trizma base, 80 mM KCl, 10 mM EDTA, 1 mM spermidine trihydrochloride, 1 mM spermine tetrahydrochloride, 0.5% Triton X-100, 0.15% (vol/vol) 2-mercaptoethanol). Cells were incubated on ice for 10 min with occasional gentle vibration and afterwards centrifuged at 2,200 g at 4 °C for 10 min. The nuclei pellet was additionally resuspended once in ice-cold nuclei isolation buffer. The supernatant was discarded and the nuclei pellet was resuspended in ice-cold 0.5 × TBE buffer. The nuclei solution was mixed with an equal amount of 1.2% (wt/vol) UltraPure™ Low Melting Point Agarose (Invitrogen) in 0.5xTBE buffer. The nuclei-agarose solution was pipetted into agarose plug molds, 100 μl per well (Bio-Rad) (2 × 10^5 cells per plug). The molds were placed at 4 °C until the agarose had gelled. The agarose gel was melted by heating the gel to a temperature of 67 °C for 10 min. The solution was cooled to 42 °C over a period of 2 min and 2 μl of β-agarase (1000 U ml^{-1}) (New England Biolabs, MA, USA) was added. The sample was incubated at 42 °C for 3 h. 500 μl 0.5 × Tris/Borate/EDTA (TBE) (Sigma-Aldrich, MO, USA) was added to the solution and the DNA stock was left to incubate for an additional 16 h at 42 °C. The DNA was stained in a 0.1 μM YOYO-1 (Invitrogen, CA, USA) solution. The solution incubated for 1 h at room temperature, followed by 1 h at 50 °C.

2.3. Chip preparation

TOPAS has a low autofluorescence [37, 38]. In order to lower this background signal even more, the chips were illuminated prior to the experiments with high intensity light. The bleaching was done by placing the polymer chip in focus on the microscope under full illumination using the same excitation wavelength (465–495 nm) as used for the experiments by simply cranking up the lamp power source at high (60 × /1.40) magnification. This was done in a step-and-repeat manner in seven pre-defined positions, in 10 min. intervals along the slit to cover the whole measurement area on the chip. In order

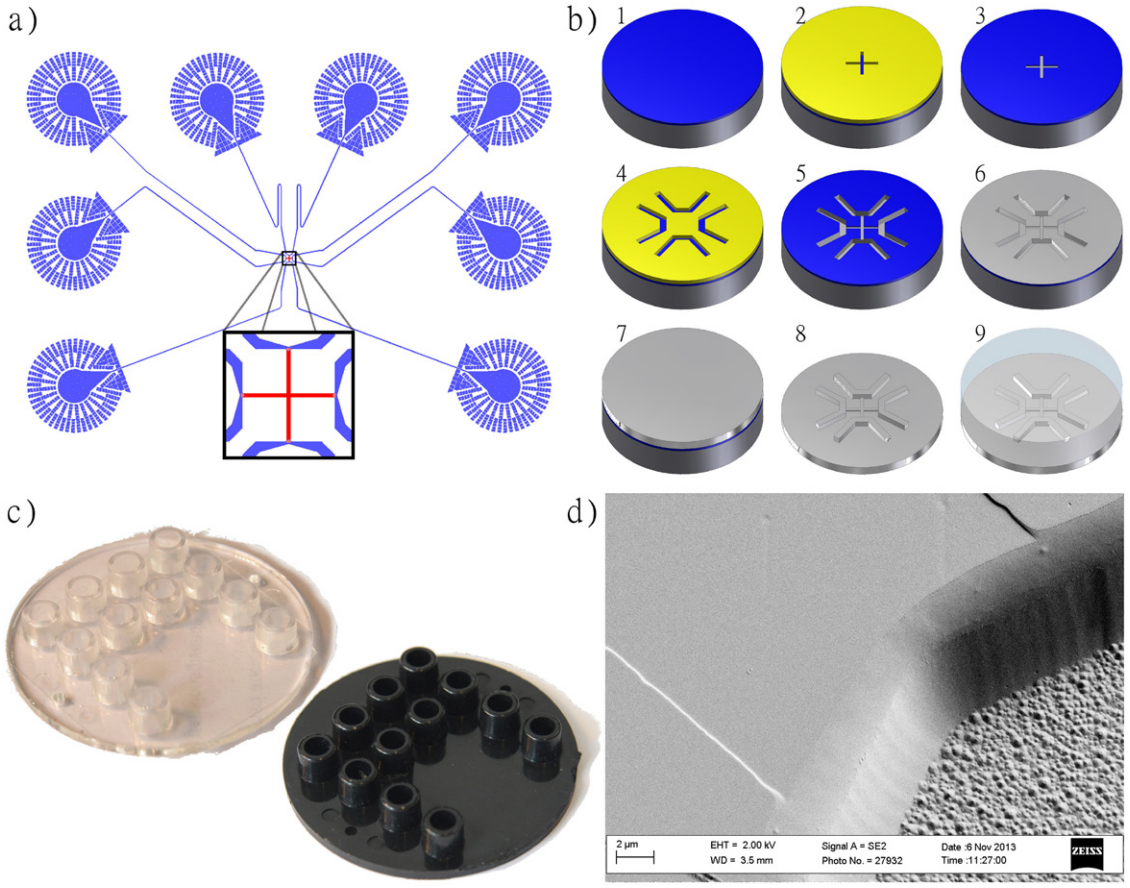

Figure 1. (a) The design used for the microfluidic system. The blue structures define the carrier channels, and the red cross (enlarged) defines the nanoslit. Support structures have been implemented around the inlets to avoid channel squeeze by pins defining the LUER ports during injection molding. (b) Production scheme for the polymer chips: 1: An oxide layer is thermally grown on a silicon wafer. 2: UV lithography is used to define the 20 μm wide, 450 μm long nanoslit. 3: An oxide specific reactive ion etch is performed, using the silicon substrate as an etch stop. 4: A second UV lithography step is used for defining the carrier channels. 5: The channels are etched using a second reactive ion etch. 6: A Ni/V seed layer is sputtered on top of the wafer. 7: The wafer is electroplated in a Ni bath. 8: Removal of the Si wafer leaves the Ni insert ready for 9: injection molding, yielding large quantities of identical polymer chips. (c) Polymer chips can be fabricated in clear polymer (left) or in black with the addition of 2% (w/w) masterbatch (right). The polymer chip contains integrated standard LUER fittings to facilitate access of a pressure controller. (d) SEM image showing the interface between the nanoslit (110 nm deep and 20 μm wide) and the carrier channel in the injection molded chip.

to document the photo-bleaching of the polymer, one image was taken every 30 s. (see figure 2) for the duration of 30 min. This significantly reduced the autofluorescence measured at 535 nm. Figure 2(a) compares autofluorescence intensities of the transparent chips fabricated in 100% COC TOPAS with intensities of chips fabricated in the same polymer but containing the 2% black masterbatch. After quenching of the autofluorescence, the final background level of intensity of the black chip reached approximately half the value of the transparent chip, and about 20% lower than the fluorescence of silica chips (figure 2(b)). The two wavelengths used here are the wavelengths proposed by *S*. Stavis for this comparison [39]. The data in figure 2(a) were fitted with the function

$$I(t) = I_\infty + I_1 \exp\left(-\frac{t}{t_1}\right) + I_2 \exp\left(-\frac{t}{t_2}\right), \qquad (1)$$

which models autofluorescence with two origins in the polymer substrate. Models involving even more terms have been proposed for polymer substrates [38], but in our case two exponential terms model the behavior of the COC TOPAS system perfectly well, we see in figure 2(a). I_∞ is the final background intensity and is shown in figure 2(b) for both polymer samples as well as for silica.

2.4. Experimental setup

To ease the filling of the microchannels and suppress photonicking, 0.5 × TBE was degassed in an ultrasonic bath for 1 h. Three buffers were prepared for the experiment. Buffer 1: 0.5 × (v/v) triton X-100 (Sigma-Aldrich), 3% (v/v) β-mercaptoethanol (BME) and 1% (v/v) 10 mg ml^{-1} Bovine Serum Albumin (BSA) (New England Biolabs) in 0.5 × TBE. Buffer 2: 2.5% (v/v) triton X-100 in Buffer 1. Buffer 3: 2% (v/v) proteinase K (Invitrogen) (20 mg ml^{-1}) in Buffer 1. The chip is wetted in a solution consisting of 7% (v/v) ethanol in the degassed 0.5 × TBE. This solution was exchanged with Buffer 2, and the chip was left for incubation at room temperature for 10 min in order for the triton X-100 and the BSA to inactivate the surface of the microchannels, thereby avoiding sticking of DNA to the walls.

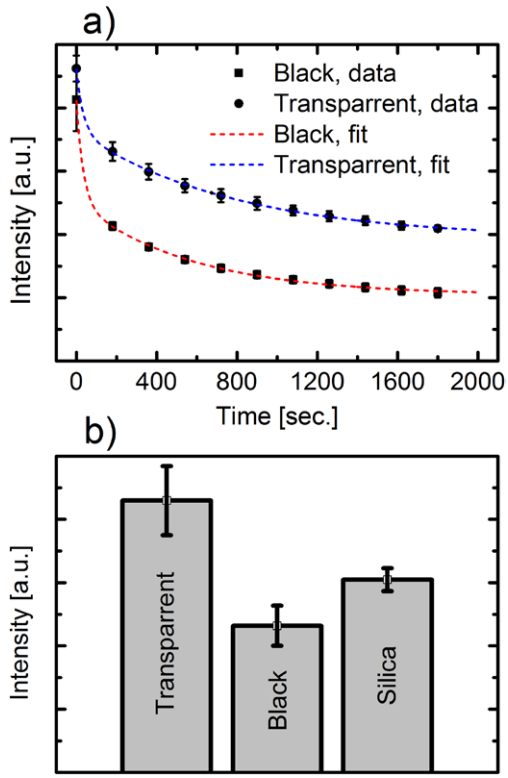

Figure 2. (a) The autoflorescence of the polymer chips as function of time during the photobleaching process. The figure shows the measured background signals with standard deviations and a fit to equation (1). For clarity, only every sixth of the measured data points are plotted. All data points were used for the fit. The error bars represent sample-to-sample variation for three samples. (b) Autofluorescence I_∞ of a black and a transparent TOPAS chip after photobleaching compared to the value for a silica chip. The error bars represent sample-to-sample variation for three samples.

After incubation, Buffer 2 was flushed out using Buffer 1. Then 3 μl DNA-solution was placed in one of the inlets along with 30 μl of Buffer 3. The remaining inlets were filled with 30 μl of Buffer 1.

Due to the thermal expansion of the polymer chip, it was impossible to heat the chip from above only, as it created too much stress in the polymer foil used as lid, which eventually broke it. We believe the shear stress in the foil spanning over the channels caused this failure mode. Instead, the DR heat cycle was performed by heating and cooling the whole chip using a flatbed PCR-machine.

The optimized on-chip handling protocol for the DR cycle comprised the following steps: (1) The chip was positioned in the flatbed PCR-machine, and a custom made aluminum piece working as a heat conductor was fitted on top of the LUER ports. The system was sealed using a PCR-foil (Microseal 'A' Film, Bio Rad). To ensure a tight seal of the LUER ports, a PMMA plate was positioned on top of the PCR-foil. The lid was closed, and (2) the temperature was raised to 55 °C for 1 h, which allowed the proteinase K to digest the histones. (3) Then the temperature was ramped up by 1° s^{-1} to a final temperature of 86 °C where the denaturation took place and the YOYO-1 fluorophore diffused away from melted AT-rich locations. This temperature was held for 10 min. (4) Afterwards the chip was cooled to 70 °C for 1 min allowing for a controlled renaturation. (5) Next, the chip was set on ice to avoid diffusion of YOYO-1 along the backbone of the molecule. The first four steps in the process are sketched in figure 3(a)).

Finally, the DNA with the DR map was stretched and imaged in the chip following the same protocol as Marie *et al* [1]. For the acquisition of data, a Nikon Eclipse microscope equipped with a 60 × NA = 1.4 objective and an additional internal 1.5 × magnification in the microscope was used.

A pressure controller (MFCS, Fluigent), connected through eight of the integrated LUER connectors in the chip, was used to manipulate the flow in order to introduce DNA into the nanoslit. Once a sufficiently long strand of DNA was positioned in the nanoslit, the flow was redirected to create a symmetrical flow (figure 3(b)), which stretched the molecule under investigation up to 95% and 100% of its contour length [1]. Images of the stretched DNA molecules were acquired with a highly sensitive electron multiplying CCD camera (Cascade II 512, Photometrics). While the DNA stretched out in the nanoslit, a script was run in the acquisition software MetaMorph (Molecular Devices), acquiring 50 images with a shutter speed of 50 ms in each of nine different fields of view. From the acquired images, the DNA was located and an average intensity along the DNA was obtained. Figure 3(c) shows a DNA molecule spanning the whole nanoslit. The inset at the bottom clearly shows the 'barcode'-like pattern.

3. Results and discussion

The economies of scale associated with injection molding lend an enormous advantage to the production method used for the devices fabricated for this work. If as few as 10 devices are fabricated, the estimated price per device amounts to roughly USD 565, with production costs including depreciation of equipment, cleanroom access time, engineering fees, and costs of materials. But if 10 000 devices are fabricated, the cost per device plunges to only ~3 USD (For calculations of the cost, see the electronic supplementary information) (stacks.iop.org/JMM/25/105002/mmedia). Moreover, the bonding process used in this work increased the yield of usable nanoslit devices from 5–10% [27] to 95%. The addition of a 2% black masterbatch to the polymer drastically reduced its fluorescence background, and thereby improved the quality of the DR map.

The low cost of the devices allowed extensive characterization of optical properties and optimization of the experimental protocol. In total, almost 1,000 chips were fabricated and used either for characterization, optimizing of protocols, or by research partners in other projects.

DNA was pipetted only once during the experiment, and was still wound around the histones while pipetted. All subsequent processes were performed on-chip, which greatly reduced the risk of fragmenting the sample DNA. This is important because our ability to handle Mb fragments reduces the influence of contamination, and because data from a continuous MB-long sequence makes its alignment to the genome more convincing. Finally, our chip-design requires the gentle procedure, was based on it: the nanoslit is 450 μm long and

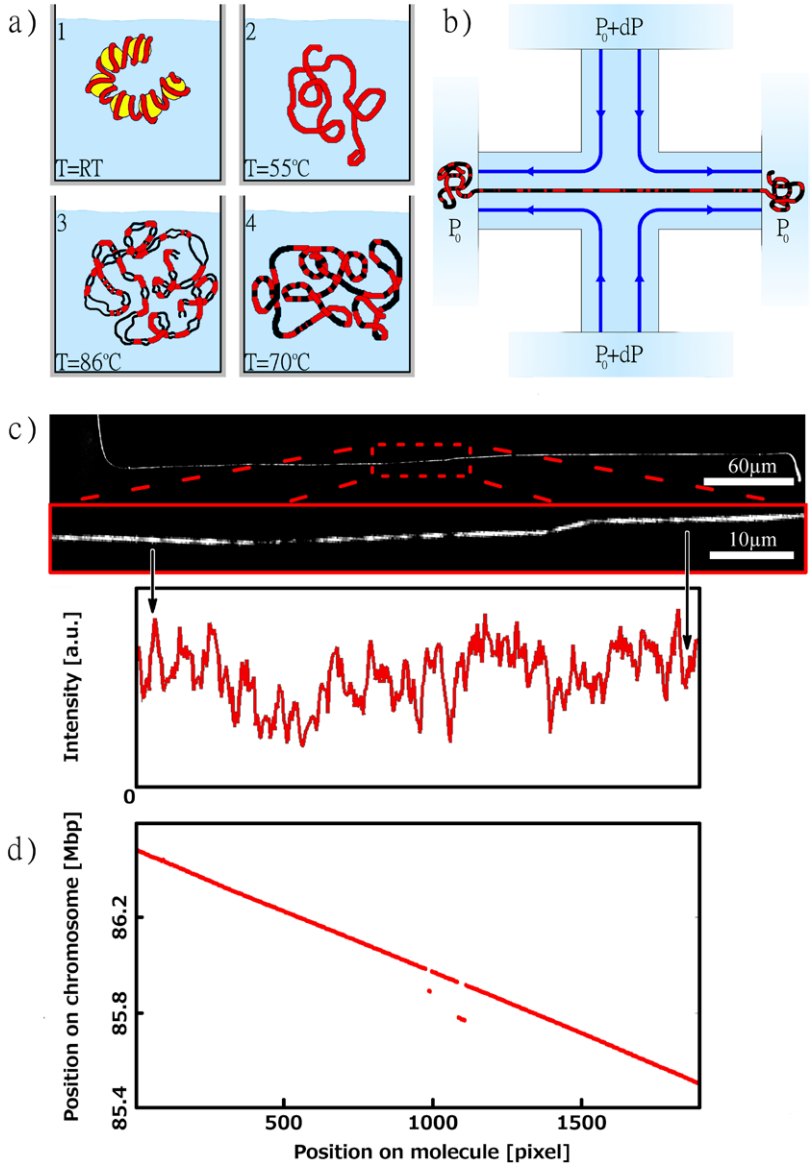

Figure 3. (a) DR maps are created by heating DNA through a series of steps on-chip. 1: At room temperature, the DNA is coiled up around the histones. 2: Adding the enzyme proteinase K and heating the sample to 55 °C for 1 h digests the histones and releases the DNA. 3: Heating the DNA to 86 °C for 10 min creates a partial denaturation of the DNA, allowing the fluorescent molecule YOYO-1 to diffuse away from the denatured locations. 4: cooling the sample to 70 °C for 10 min results in a controlled renaturation, ensuring constant mechanical properties along the backbone. (b) The denatured–renatured DNA is stretched out in the nanoslit. Applying pressure from top and bottom creates a flow that stretches out the DNA to almost 100%. (c) The DR map was acquired with an optical microscope, and the intensity profile along the molecule was extracted. (d) The acquired DR map is mapped to chromosome 16 between the positions ~85.5 Mbp and ~86.5 Mbp

therefore requires DNA molecules longer than 1.4 Mb in order to work as intended. A shorter molecule cannot span the entire nanoslit and hence is exposed to unequal opposing drag forces, which cause the molecule to drift during data acquisition. For DR mapping to provide long-range context for the short read lengths of NGS, it is also a significant advantage to have large continuous fragments of the genome.

In total 24 molecules were stretched and imaged in the black polymer devices. The DR maps from these molecules were mapped against a theoretical DR map found using Bubblyhelix (www.bubblyhelix.org) [41] and the human reference genome hg18, with the algorithm described in the supporting information of Marie *et al* [1]. Figure 3(d) shows an example of the acquired data mapped against a part of chromosome 16. The agreement is excellent.

Out of the 24 molecules, 20 of them were successfully mapped to positions in the human reference genome. In the supporting information of this manuscript we explain in detail how the mapping is done, and we show all 20 mapped sequences. The rest did not match anywhere, which can be the consequence of several factors. In the human genome, 5–10% remains unannotated (the centromeres, pericentric heterochromatin, and short p-arms of the five acrocentric chromosoms)[4]

[4] Incorporating known polymorphisms in the reference genome [references to: www.ncbi.nlm.nih.gov/dbvar/ and www.ncbi.nlm.nih.gov/SNP/ (assessed 2015-03-27)] potentially gives an even higher fraction of mapped molecules.

Thus, 10–15% of the human genome is unmapped, which results in, on the average, 2.4 to 3.6 out of 24 randomly picked pieces of DNA being unmappable. The probabilities of getting four or more unmapped molecules out of 24 are in the range 0.21–0.50, see the electronic supplementary information (stacks.iop.org/JMM/25/105002/mmedia). This constitutes the far most probable reason for our unmappable DNA fragments, although the true experimental error rates were not explicitly tested. These could be investigated independently by covering a small genome (as, e.g. *E*scherichia *coli*).

Other factors could be large-scale structural variations and copy number variants in these molecules compared to the reference genome. Finally, the data quality might not be sufficient for these few molecules, e.g. due to drift and other experimental artifacts. Contamination with bacterial DNA used in adjacent labs is also a possibility, but contamination of the sample by microorganisms leading to four out of 24 analyzed molecules originating from the contaminant is so dramatic that it most likely would be detected during the sample preparation, considering the difference in genome size between human cells and, say, yeast or *E. coli*.

Finally, it would require the mapping of ~9600 1 Mb-long DNA molecules to cover 95% of the base pairs in the human genome at least once [41]. This could be done within a reasonable amount of time, if the research-scale experimental setup used in the present analysis was replaced by a fully automated setup.

4. Conclusion

We have demonstrated single-molecule DNA mapping of human chromosomal DNA on cheap, disposable polymer devices. This has been done on chips with a price per device as low as 3 USD and high-yield production potential allowing several thousands of chips to be produced within a few days.

The background fluorescence signal of the polymer devices was reduced significantly by the addition of a black masterbatch in the polymer material and quenching the autofluorescence by irradiation with intensive light with the same wavelength as used for excitation of the dye used in the experiments.

An optimized on-chip handling protocol comprising the steps of DNA extraction, denaturation, renaturation, and stretching of the DNA was developed and allowed a considerable reduction of the risk of fragmenting the DNA during experiments.

DNA was positioned in the 450 μm-long nanoslits and stretched out to more than 95% of the contour length of the molecule. This allowed imaging of more than 1.4 Mb of the human genome in a single data acquisition.

Out of 24 molecules considered for mapping in this particular validation study, 20 were mapped to DR profiles calculated from the human reference genome. It is plausible that the remaining four molecules could not be mapped due to unsequenced regions in the reference genome, although other reasons are possible.

The demonstrated polymer chip platform has a big potential for optical mapping of individual DNA molecules for use as a complimentary method to next-generation sequencing. Moreover, the platform performs as well as silica devices without their long production time with low yield and prohibitively high cost. Thus, the presented approach will enable users with limited experience to use this sophisticated optical mapping method in conjunction with other methods, thereby saving time and money.

Acknowledgments

This work was supported by the *Danish Council for Strategic Research* through the Strategic Research Center PolyNano (grant no. 10-092322/DSF) and from the *Danish Agency for Science, Technology and Innovation* through DELTA's performance contract, CiPOC (grant no. 10-076609). We thank Dr Lis Hasholt's group (Section for Neurogenetics, Department of Cellular and Molecular Medicine, University of Copenhagen) for the fibroblast cell line used in the project (Danish Data Agency, 2013-54-0582).

References

[1] Marie R *et al* 2013 Integrated view of genome structure and sequence of a single DNA molecule in a nanofluidic device *Proc. Natl Acad. Sci. USA* **110** 4893–8
[2] Buermans H P J and den Dunnen J T 2014 Next generation sequencing technology: advances and applications *Biochim. Biophys. Acta (BBA)—Mol. Basis Dis.* **1842** 1932–41
[3] Samad A H *et al* 1995 Mapping the genome one molecule at a time—optical mapping *Nature* **378** 516–7
[4] Aston C, Mishra B and Schwartz D C 1999 Optical mapping and its potential for large-scale sequencing projects *Trends Biotechnol.* **17** 297–302
[5] Schwartz D C, Li X J, Hernandez L I, Ramnarain S P, Huff E J and Wang Y K 1993 Ordered restriction maps of *saccharomyces cerevisiae* chromosomes constructed by optical mapping *Science* **262** 110–4
[6] Zhou S *et al* 2007 Validation of rice genome sequence by optical mapping *BMC Genomics* **8** 278
[7] Latreille P *et al* 2007 Optical mapping as a routine tool for bacterial genome sequence finishing *BMC Genomics* **8** 321
[8] Dong Y *et al* 2013 Sequencing and automated whole-genome optical mapping of the genome of a domestic goat (Capra hircus) *Nat. Biotechnol.* **31** 135–41
[9] Levy-Sakin M and Ebenstein Y 2013 Beyond sequencing: optical mapping of DNA in the age of nanotechnology and nanoscopy *Curr. Opin. Biotechnol.* **24** 690–8
[10] Levy-Sakin M *et al* 2014 Toward single-molecule optical mapping of the epigenome *ACS Nano* **8** 14–26
[11] Reisner W *et al* 2010 Single-molecule denaturation mapping of DNA in nanofluidic channels *Proc. Natl Acad. Sci. USA* **107** 13294–9
[12] Teng C *et al* 2015 Whole-genome optical mapping and finished genome sequence of sphingobacterium deserti sp nov., a new species isolated from the Western Desert of China *Plos One* **10** e0122254
[13] Welch R L, Sladek R, Dewar K and Reisner W W 2012 Denaturation mapping of *S. cerevisiae Lab Chip* **12** 3314–21

[14] Berard D J *et al* 2014 Convex lens-induced nanoscale templating *Proc. Natl Acad. Sci. USA* **111** 13295–300
[15] Flyvbjerg H 2014 How to get into that 'room at the bottom' *Proc. Natl Acad. Sci. USA* **111** 13249–50
[16] Mardis E R 2006 Anticipating the $1,000 genome *Genome Biol.* **7**
[17] Service R F 2006 Gene sequencing—The race for the $1000 *Genome Sci.* **311** 1544–6
[18] Becker H 2009 Chips, money, industry, education and the 'killer application' *Lab Chip* **9** 1659–60
[19] Becker H 2009 It's the economy *Lab Chip* **9** 2759–62
[20] Elders J, Jansen H V, Elwenspoek M and Ehrfeld W 1995 IEEE DEEMO: a new technology for the fabrication of microstructures *IEEE Proc. Micro Electro Mechanical Systems (New York)* pp 238–43
[21] McCormick R M, Nelson R J, AlonsoAmigo M G, Benvegnu J and Hooper H H 1997 Microchannel electrophoretic separations of DNA in injection-molded plastic substrates *Anal. Chem.* **69** 2626–30
[22] Utko P, Persson F, Kristensen A and Larsen N B 2011 Injection molded nanofluidic chips: fabrication method and functional tests using single-molecule DNA experiments *Lab Chip* **11** 303–8
[23] Ostergaard P F, Matteucci M, Reisner W and Taboryski R 2013 DNA barcoding via counterstaining with AT/GC sensitive ligands in injection-molded all-polymer nanochannel devices *Analyst* **138** 1249–55
[24] Chantiwas R *et al* 2011 Flexible fabrication and applications of polymer nanochannels and nanoslits *Chem. Soc. Rev.* **40** 3677–702
[25] Wu J H, Chantiwas R, Amirsadeghi A, Soper S A and Park S 2011 Complete plastic nanofluidic devices for DNA analysis via direct imprinting with polymer stamps *Lab Chip* **11** 2984–9
[26] Chantiwas R *et al* 2010 Simple replication methods for producing nanoslits in thermoplastics and the transport dynamics of double-stranded DNA through these slits *Lab Chip* **10** 3255–64
[27] Tanzi S *et al* 2012 Fabrication of combined-scale nano- and microfluidic polymer systems using a multilevel dry etching, electroplating and molding process *J. Micromech. Microeng.* **22**
[28] Chen Q, Yang L, Wang Z and Liu Z 2010 Influence of the solution on adhesion layer polymerized in radio frequency pulsed plasma for DNA hybridization assay *IEEE Trans. Plasma Sci.* **38** 1897–902
[29] Tandon V, Bhagavatula S K and Kirby B J 2009 Transient zeta-potential measurements in hydrophobic, TOPAS microfluidic substrates *Electrophoresis* **30** 2656–67
[30] Das S K, Austin M D, Akana M C, Deshpande P, Cao H and Xiao M 2010 Single molecule linear analysis of DNA in nano-channel labeled with sequence specific fluorescent probes *Nucleic Acids Res.* **38**
[31] Lam E T *et al* 2012 Genome mapping on nanochannel arrays for structural variation analysis and sequence assembly *Nat. Biotechnol.* **30** 771–6
[32] Kim Y *et al* 2011 Nanochannel confinement: DNA stretch approaching full contour length *Lab Chip* **11** 1721–9
[33] Andresen K O *et al* 2010 Injection molded chips with integrated conducting polymer electrodes for electroporation of cells *J. Micromech. Microeng.* **20**
[34] Tanzi S *et al* 2013 Ion channel recordings on an injection-molded polymer chip *Lab Chip* **13** 4784–93
[35] Matteucci M, Christiansen T L, Tanzi S, Ostergaard P F, Larsen S T and Taboryski R 2013 Fabrication and characterization of injection molded multi level nano and microfluidic systems *Microelectron. Eng.* **111** 294–8
[36] Zhang M, Zhang Y, Scheuring C F, Wu C-C, Dong J J and Zhang H-B 2012 Preparation of megabase-sized DNA from a variety of organisms using the nuclei method for advanced genomics research *Nat. Protocols* **7** 467–78
[37] Hawkins K R and Yager P 2003 Nonlinear decrease of background fluorescence in polymer thin-films—a survey of materials and how they can complicate fluorescence detection in mu TAS *Lab Chip* **3** 248–52
[38] Piruska A *et al* 2005 The autofluorescence of plastic materials and chips measured under laser irradiation *Lab Chip* **5** 1348–54
[39] Stavis S M 2012 A glowing future for lab on a chip testing standards *Lab Chip* **12** 3008–11
[40] Tostesen E, Liu F, Jenssen T K and Hovig E 2003 Speed-up of DNA melting algorithm with complete nearest neighbor properties *Biopolymers* **70** 364–76
[41] Clarke L and Carbon J 1976 Colony bank containing synthetic Col El hybrid plasmids representative of entire *E. coli* genome *Cell* **9** 91–9